Accepted Manuscript

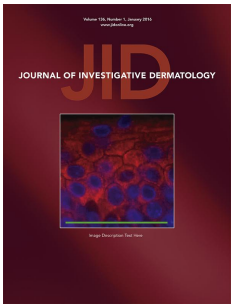

CD271 downregulation promotes melanoma progression and invasion in 3-dimensional models and in zebrafish

Annalisa Saltari, Francesca Truzzi, Marika Quadri, Roberta Lotti, Elisabetta Palazzo, Giulia Grisendi, Natascia Tiso, Alessandra Marconi, Carlo Pincelli

PII: S0022-202X(16)31351-3

DOI: 10.1016/j.jid.2016.05.116

Reference: JID 385

To appear in: *The Journal of Investigative Dermatology*

Received Date: 29 January 2015

Revised Date: 23 May 2016

Accepted Date: 31 May 2016

Please cite this article as: Saltari A, Truzzi F, Quadri M, Lotti R, Palazzo E, Grisendi G, Tiso N, Marconi A, Pincelli C, CD271 downregulation promotes melanoma progression and invasion in 3-dimensional models and in zebrafish, *The Journal of Investigative Dermatology* (2016), doi: 10.1016/ j.jid.2016.05.116.

CD271 downregulation promotes melanoma progression and invasion in 3-dimensional models and in zebrafish

Annalisa Saltari[1*], Francesca Truzzi[1*], Marika Quadri[1], Roberta Lotti[1], Elisabetta Palazzo[1], Giulia Grisendi[2], Natascia Tiso[3], Alessandra Marconi[1] and Carlo Pincelli[1]

[1]Laboratory of Cutaneous Biology, Department of Surgical, Medical, Dental and Morphological Sciences, University of Modena and Reggio Emilia, Modena, Italy

[2]Laboratory of Cell Biology and Advanced Cancer Therapies, Department of Medical and Surgical Sciences for Children & Adults, University of Modena and Reggio Emilia, Modena, Italy

[3]Laboratory of Developmental Genetics, Department of Biology, University of Padova, Padova, Italy

[*] These authors contributed equally to the work

Corresponding author:

Carlo Pincelli,

Laboratory of Cutaneous Biology, Department of Surgical, Medical, Dental and Morphological Sciences,

University of Modena and Reggio Emilia, Via Del Pozzo 71, 41124 Modena, Italy.

Tel: +39 059 4222931; FAX: +39 059 4224271;

e-mail: carlo.pincelli@unimore.it

Short title: Role of CD271 in melanoma progression

Abbreviations: Neurotrophins (NTs), radial growth phase (RGP), vertical growth phase (VGP), 3dimensional (3D), days post injection (dpi), days post fertilization (dpf)

ABSTRACT

CD271 is a neurotrophin receptor variably expressed in melanoma. While contradictory data are reported on its role as a marker of tumor initiating cells, little is known on its function in tumor progression. CD271 expression was higher in spheroids derived from freshly isolated cells of primary melanomas and in primary WM115 and WM793-B cell lines, while it decreased during progression to advanced stages in cells isolated from metastatic melanomas and in metastatic WM266-4 and 1205Lu cell lines. Moreover, CD271 was scarcely detected in the highly invasive spheroids (SKMEL28 and 1205Lu). CD271, originally expressed in the epidermis of skin reconstructs, disappeared when melanoma started to invade the dermis. SKMEL8 $CD271^{-}$ cells showed greater proliferation and invasiveness in vitro, and were associated with a higher number of metastases in zebrafish, as compared to $CD271^{+}$ cells. CD271 silencing in WM115 induced a more aggressive phenotype in vitro and in vivo. On the contrary, CD271 overexpression in SKMEL28 cells reduced invasion in vitro, and CD271 overexpressing 1205Lu cells was associated with a lower percentage of metastases in zebrafish. A reduced cell-cell adhesion was also observed in absence of CD271. Taken together, these results indicate that CD271 loss is critical for melanoma progression and metastasis.

INTRODUCTION

Melanoma is the deadliest type of skin cancer and its incidence is rising faster than any other solid tumour (Eggermont et al., 2014). While early melanomas can be cured by surgical excision, metastatic melanomas are generally fatal due to their resistance of current chemotherapies (Gray-Shopfer et al., 2007) Melanoma arises from a precursor, enters in the radial growth phase (RGP) with cells proliferating in the epidermis, invades the dermis and start the vertical growth phase (VGP). We have previously shown that melanoma cells express neurotrophins (NTs) and their receptors, and play a role in tumor progression (Truzzi et al., 2008). NTs bind two classes of

receptors: the high affinity receptors (Trks) and the low affinity receptor ($p75^{NTR}$ or CD271). CD271 was firstly isolated from a melanoma cell line and is expressed on neural crest cells from which melanocytes are derived (Kruger et al., 2002). It belongs to the TNF receptor superfamily and mediates apoptosis in different cell settings via its own signaling pathway (Kraemer et al., 2014; Truzzi et al., 2011; Blöchl and Blöch, 2007). The interaction of apoptosis related protein APR-1 with CD271 activate apoptosis in melanoma cells (Selimovic et al., 2012) . CD271 activation mediates apoptosis in bladder and prostate cancer (Khwaja et al., 2004). In addition, CD271 is hardly detected in invasive cutaneous squamous cell carcinoma (Dallaglio et al., 2014). In the last few years, contradictory results concerning CD271 as a marker of melanoma initiating cells (MICs) have been pubblished. It has been recently proposed that CD271 is an "imperfect marker" for MICs, as fast growing/$CD271^+$ cells exhibit poor tumorigenic ability (Cheli et al., 2014). To better understand the role of this receptor in melanoma, we studied CD271 in vitro by using 3-dimensional (3D) multicellular spheroids and skin equivalents which closely mimick the behavior of solid tumors in vivo (Griffith and Swarz, 2006). We demonstrate the $CD271^-$ spheroids proliferate and invade more than $CD271^+$ spheroids. CD271 silencing induces both cell migration and proliferation, which are reduced when CD271 is overexpressed. Moreover, using a zebrafish melanoma model, we provide evidence that lack of CD271 is critical for melanoma progression, being associated with a higher number of metastases. Finally, we show a reduced expression of β_1-integrin and a decreased cell-cell adhesion in absence of CD271, resulting in a poor tumor cell adhesion and in a greater predisposition to invade the microenvironment.

RESULTS

CD271 inversely correlates with melanoma progression stage and invasiveness in 3D spheroids.

We recently demonstrated that CD271 is markedly expressed in early stage melanomas, while it is progressively lost during tumor progression, showing an inverse correlation with hypoxia

inducible factor-1 (HIF-1α) (Marconi et al., 2015). Given this finding, we decided to study the role of CD271 in spheroids that mimic the 3D architecture and heterogeneity of melanoma (Beaumont et al., 2014). CD271 expression was evaluated in long-standing cell lines (WM115, WM266-4, SKMEL28, WM793-B and 1205Lu) derived from melanomas of different stages and in cells freshly isolated from a primary (PM) and a metastatic melanoma (MM).

CD271 significantly decreases in MM, as compared to the primary melanoma (PM) derived from the same patient (Figure 1A). The same behaviour is observed in the long-standing cell lines: primary WM115 and WM793-B cells express higher levels of CD271 than their metastatic counterparts (WM266-4 and 1205Lu, respectively). CD271 levels in the primary tumors were highly variable (WM115, SKMEL28, WM793-B and PM), thus mirroring the great inter-patient heterogeneity of this tumor. The same heterogeneity was observed in the metastases (WM266-4, 1205Lu and MM). It should be noted that the levels of CD271 is significantly higher in WM266-4 cell line derived from a dermal metastasis, than in 1205Lu and MM cells that originate from lung metastasis. Furthermore, the percentage of the melanoma predictor of proliferation Ki67 is higher in cells expressing the lowest levels of CD271 (SKMEL28, 1205Lu and MM) (Figure 1B). To confirm the ability of spheroids to reflect the behaviour of tumor in vivo, cells isolated from primary melanomas were seeded and chatacterized in vitro. Markers of melanoma (HIF-1-α, CD271, ABCB5 and Oct4) are maintained in spheroids up to 168h and they are comparable to those observed in skin lesion and in cells freshly isolated from the same patient (Figure 1C and 1D). Finally, MM spheroids proliferate more than PM spheroids as shown by MTT (Figure 1E), replicating the growth of the tumor in vivo. Spheroids were then implanted into a matrix of collagen I which mimics the tumor microenvironment (Figure 1F). Areas occupied by the cells reveales greater invasion abilities in MM than in PM spheroids (Figure 1G). Confocal microscopy confirmed that CD271 (green) is barely detectable in SKMEL28 and 1205Lu spheroids (Figure 1H), as also shown by western blotting (Figure 1I). Indeed, survivin and Notch1, involved in

melanoma progression, are more expressed in SKMEL28, WM793-B and 1205Lu cells than in less aggressive cell lines. In addition, active caspase-3, which promotes migration and invasion of non apoptotic melanoma cells (Liu et al., 2013), is higher in SKMEL28 and 1205Lu than in the other spheroids. HIF-1α is higher in spheroids derived from advanced stage melanomas (WM266-4 and 1205Lu) (Figure 1I). In addition, metastatic WM266-4 and 1205Lu spheroids invade more than their primary counterparts (WM115 and WM793-B, respectively) (Figure 1L,M), and spheroids expressing the lowest levels of CD271 (SKMEL28 ans 1205Lu), display the greatest invasive phenotype (Figure 1M). These data indicate that CD271 inversely correlates with melanoma progression and in vitro invasiveness.

CD271 is associated with poor invasiveness in spheroids and skin equivalents

To evaluate the role of CD271 in melanoma invasiveness, spheroids were transferred into collagen I, and CD271 expression was evaluated by immunohistochemistry. In all cell lines, the majority of $CD271^+$ cells are non-invasive (Figure 2A). Consistently, cells expressing CD271 remain mostly confined to the body of the sphere (Figure 2B). The majority of invading cells are $CD271^-$, indicating a greater predisposition to invade the microenvironment (Figure 2C). To confirm these data in a model that better reflects the in vivo tissue architecture, cells were used to generate 3D skin equivalents. Melanoma reconstructs recapitulate tumor pathology, as shown by H&E and S100 staining (Figure 2D). WM115 and WM266-4 cells are confined to the epidermis, while SKMEL28, WM793-B and 1205Lu cells localize at the dermal-epidermal junction at 6 days after plating. All melanoma cells invade the dermis at 12 days after seeding. At day 6, CD271 expression is detected only in WM115, WM266-4 and WM793-B derived reconstructs, while it decreases or disappeares during progression to 12 days in skin equivalents originated from the same cell lines. By contrast, CD271 is not expressed in reconstructs derived from SKMEL28 and 1205Lu cells either at 6 or 12 days (Figure 2D). Taken together, these data confirm an inverse correlation between CD271 receptor and melanoma invasiveness.

CD271$^-$ spheroids display increased proliferation and invasion abilities

To better understand the role of CD271 in melanoma, we isolated SKMEL28 CD271$^+$ and CD271$^-$ cells (Figure S1A, B) that were seeded as spheroids (Figure S2A). CD271 $^+$ spheroids proliferate significantly less than CD271$^-$ spheroids from 72 up to 168 h (Figure 3A). Analysis of pictures (Figure 3B) revealed that the area of CD271$^-$ spheroids increases in a time -dependent manner, whereas it remains unchanged in CD271$^+$ spheroids (Figure 3C). Given that CD271 is used as a marker of cancer stem cells, the possibility that CD271$^-$ cells exhaust earlier than CD271$^+$ cells was also evaluated: spheroids were grown for 7 days, dissociated, counted and replated under the same conditions in a long-term assay. Despite both CD271$^-$ and CD271$^+$ spheroids propagate during serial passages, the number of cells derived from CD271$^-$ spheroids is always higher than those from CD271$^+$ spheroids (Figure 3D). On the other hand, 30% of CD271$^+$ spheroids express the pluripotency marker Oct4, while its expression is absent in CD271$^-$spheroids (Figure 3E). WM793-B cells were also sorted (Figure S1C, D) and cultured as 3D spheroids (Figure S2C). The calculation of areas (Figure S2D, E), MTT (Figure S2F), long term growth (Figure S2G) and Oct4 levels (Figure S2H) yielded the same findings. SKMEL28 spheroids were then implanted into type I collagen and monitored (Figure S2B). CD271$^-$ spheroids invade significantly more than CD271$^+$ spheroids. Factor shape and percentage of fragmentation, two values correlated with melanoma invasiveness, are higher in CD271$^-$ than in CD271$^+$ spheroids (Figure 3F). In addition, CD271$^-$ spheroids occupy a greater area (Figure 3G) and display a higher number of invading cells (Figure 3H) than their positive counterpart. The calculation of the distance revealed that CD271$^-$ spheroids achieve greater distances than CD271$^+$ cells in collagen at 96 and 120 h (Figure 3I). Consistently, the epithelial-mesenchymal transition factor Slug, that promotes melanoma invasion (Fenouille et al., 2012), is more expressed in CD271$^-$ cells. Results are confirmed in WM793-B cells (Figure S2I, L, M and N).

CD271 silencing enhances proliferation and invasiveness in melanoma spheroids

To evaluate whether the absence of CD271 was responsible for a more aggressive phenotype in vitro, we silenced CD271 in WM115 cells, which express high level of the receptor (Figure 4A). Transfected cells were seeded to obtain spheroids (Figure S3A). First, following CD271 silencing, survivin increases, as a function of increased aggressiveness (Figure 4A). Image analysis (Figure 4B) revealed higher areas in CD271 silenced spheroids up to 120 h, as compared to scramble cells (Figure 4C), indicating an increased proliferation, as confirmed by MTT (Figure 4D). CD271 silencing yelded the same results in WM793-B cells (Figure S3B, C, D, F).

24 h after implantation into collagen I, CD271 silencing induces a marked change in spheroids, that appear disgregated into single cells, as compared to scrambled cells (Figure 4E). This reflects a greater invasiveness, as shown by the increase in factor shape, percentage of fragmentation (Figure 4F) and total area (Figure 4G). Moreover, CD271 silencing results in a higher number of cells invading type I collagen (Figure 4H) and reaching higher distances than controls (Figure 4I). Taken together, these data suggest that lack of CD271 is associated with greater proliferation and invasion ability.

CD271 overexpression decreases tumor proliferation and invasiveness in melanoma spheroids

Because the absence of CD271 correlates with greater invasion and proliferation, we asked whether its overexpression could revert melanoma to a less aggressive phenotype. To this purpose, SKMEL28 were infected with a CD271 or mock viral vector, and spheroids were monitored (Figure S4A). First, CD271 overexpression causes a downregulation of the markers of invasion Slug and caspase-3 (Figure 5A). Pictures (Figure 5B) reveal a slight decrease in the total areas occupied by CD271 infected spheroids (Figure 5C). Moreover, CD271 overexpressing spheroids proliferate significantly less than mock cells (Figure 5D). Given that CD271 receptor mediates apoptosis in many cell settings, we evaluated whether the reduced viability was

associated with the activation of the apoptotic cascade. Yet, the percentage of apoptotic cells failed to increase in CD271 overexpressing cells (Figure 5E, F). CD271 overexpressing spheroids were then implanted into collagen I (Figure S4B), displaying a reduced invasiveness, as shown by the decrease in factor shape and percentage of fragmentation (Figure 5G). Consistently, the total area (Figure 5H) and the area of invasion are significantly reduced in CD271 overexpressing spheroids, as compared to control (Figure 5I). Finally, they reach a lower distance in collagen I than mock spheroids (Figure 5L). The same results were obtained by infecting 1205Lu cell line (Figure S4C, D, E, F, G, H, I).

The lack of CD271 favours tumor metastasis in zebrafish and is associated with a reduced cell-cell adshesion

The zebrafish model has recently contributed to major insights in the progression of melanoma (White et al., 2013; Kaufman et al., 2016). In order to definitely confirm the role of CD271 in melanoma, we evaluated the ability of zebrafish in mirroring the metastatic process. Primary WM115 and metastatic 1205Lu cells (red) were injected into transparent larvae and the spread of cells was evaluated 6 days later (Figure S5A,B). Larvae were xenotraplanted under three different conditions: 1) $CD271^+$ and $CD271^-$ cells sorted from SKMEL28 cell lines (Figure 6A-D); 2) WM115 cells silenced for CD271 (Figure 6E-G) and 3) CD271 overexpressing 1205Lu cells (Figure 6H-L). At day 2, cells are confined to the site of injection (yolk), while at day 6/7 post injection (dpj), the number of metastases is markedly increased in SKMEL $CD271^-$ cells (Figure 6 A,B) and in WM115 CD271 silenced cells (Figure 6E, F) as compared to $CD271^+$ and control cells, respectively. The same result is observed when SKMEL28 $CD271^+$ (green) and $CD271^-$ (red) cells where injected together (Figure 6D). On the contrary, the percentage of metastases decreases at 6 dpj of CD271 overexpressing 1205Lu (Figure 6H,I). A higher number of “full” (>10 cells) and “medium” (5-10 cells) metastases are observed in absence of CD271, while

zebrafish injected with SKMEL28 CD271^{+} (Figure 6C), WM115 scramble (Figure 6G), and CD271 infected 1205Lu cells (Figure 6L) display mostly "initial metastasis" (2-4 cells),.

Finally, to better understand the mechanism underlying the role of CD271 in melanoma progression, we hypothesized a correlation between adhesion molecules and CD271 levels. The observation that CD271 silencing in WM115 spheroids (Figure 4) associates with a less compact shape, suggests that the lack of CD271 could be related to a decrease in cell-cell adhesion, thus increasing the predisposition to invade. We show that β_1-integrin is reduced in the metastatic WM266-4 and 1205Lu cells (Figure 6M). In addition, CD271 silencing causes β_1-integrin downregulation, while CD271 overexpression correlates with increased levels of the protein (Figure 6N). Finally, CD271 silenced WM115 cells display a reduced inter-cellular adhesion, as shown by the reduced number of adherent cells (red), while increased adhesion is observed in CD271 overexpressing 1205Lu cells (Figure 6O). These results demonstrate that the lack of CD271 favours tumor metastasis in vivo, and that CD271 is correlated with cell-cell adhesion.

DISCUSSION

The present study provides a number of data that shed light on the function of CD271 in melanoma progression. Using 3D spheroids, we demonstrate that CD271 is inversely correlated to the invasiveness and growth of the tumor. CD271 decreases during progression from primary to metastatic melanoma of the same patient. When spheroids are implanted into a matrix of collagen I, CD271 is highly expressed in cells confined to the body of the sphere, while it is almost absent in cells that detach from the sphere to invade. These results seem to be in contrast with previous publications reporting a role of NTs in mediating melanoma cell invasion and migration (Marchetti et al., 1998; Truzzi et al., 2008). Because early studies were carried out in 2D cultures, we hypothesize that the conflicting results are due to the different systems. Multicellular spheroids mimic the 3D architecture and heterogeneity of melanoma by recreating the oxygen/nutrients gradient (Beaumont et al., 2014). Moreover, genomic profile of glioma is

preserved in spheroids but not in primary monolayer cultures (De Witt et al., 2009), while 3D models markedly affect gene expression in melanoma (Ghosh et al., 2005). Skin reconstructs are a good tool for studying tumor-microenvironment interactions (Vorsmann et al., 2013). Here, we show that CD271 is expressed in melanoma cells located in the epidermis of skin reconstructs, while it disappeares when melanoma invades the dermis. Consistently, HIF-1α is present at great levels in tumors invading the dermis, while CD271 is markedly expressed in early stage melanomas, and it is progressively lost during progression (Marconi et al., 2015).

Contradictory results concerning CD271 and its use as a marker to isolate MICs have been recently published. Boiko (2010) demonstrated that MICs can be isolated as a highly enriched CD271 population. Moreover, CD271/Sox10-positive melanoma cells have been associated with higher metastatic potential (Civenni et al., 2011). On the contrary, melanoma can metastasize in mice irrespective of whether they derive from $CD271^+$ or $CD271^-$ cells (Quintana et al., 2010). In the present paper, we demonstrate that $CD271^+$ cells are slow-growing cells and display increased levels of the stemness gene Oct4. On the other hand, both $CD271^+$ and $CD271^-$ spheroids display a long term growth. Moreover, CD271 is regulated by hypoxic and stringent culture conditions (Menon et al., 2015), and its detectability is affected by the tumor digestion protocol. Most studies were carried out in spheroids maintained in a stem cell medium that select a subpopulation with stemness proprierties (Ramgolam et al., 2011). Here, spheroids were obtained according to the liquid overlay method that preserves tumor heterogeneity. Finally, biopsies were processed with a protocol that avoids the damage of surface epitopes. In substance, although the current paper did not aim to fully address the correlation between CD271 and MICs, the high percentage of $CD271^+$ cells in primary melanomas seems to rule out their stem nature. Whether a subpopulation of $CD271^+$ cells could contain MICs remains to be determined.

The inverse correlation between CD271 expression and melanoma progression was further confirmed by using a zebrafish model. The zebrafish has recently emerged as an important model in cancer research able to develop human tumors, with similar morphology and comparable

signaling pathways (Heilmann et al., 2015; Kaufman et al., 2016). In the present work, we demonstrate that the lack of CD271 is critical for melanoma progression in vivo. When injected into zebrafish, CD271 silenced WM115 cells, SKMEL28 CD271$^-$ cells and 1205Lu mock cells provoked a higher number of metastases as compared with cells expressing higher amounts of CD271. Consistently, spheroids acquire a more invasive phenotype in absence of CD271, as also demonstrated by the increase of Slug and Caspase 3 levels. Because SKMEL28 spheroids fail to undergo apoptosis after CD271 overexpression, the activation of caspase-3 is consistent with its ability to promote invasion (Liu et al., 2013; Donato et al., 2014).

CD271 silencing downregulates β_1-integrin and reduced cell-cell adhesion, while its overexpression in 1205Lu induces β_1-integrin upregulation and an increase in cell-cell adhesion. It is known that $\alpha_4\beta_1$-integrin inhibits metastases, and it is involved in the intercellular adhesion (Quian et al., 1994). Moreover, Slug is associated with loss of cell-cell adhesion mediated by E-cadherin in melanoma (Shirley et al., 2012). This suggests that CD271 downregulation promotes melanoma progression and invasion at least in part because of the lack of cell-cell adhesion. However, further experiments are required to identify the molecules that take part in this process. In conclusion, we hypothesize that a melanoma subpopulation needs to turn off CD271 to acquire the ability to invade during early stages of melanoma progression.

MATERIALS & METHODS

Cell culture

WM115, WM266-4, SKMEL28, WM793B and 1205Lu (ATCC, Manassas, VA, USA) were cultured as indicated by the manufacturer. MTT, liquid overlay method, invasion assay, picture analysis and long term were performed as indicated in Supplementary Materials. Melanoma biospies were processed as described in Supplementary materials.

FACS

Spheroids incubated with anti CD271 antibody (1:100 in PBS, Lab Vision Corporation, Thermo Fisher Scientific, Fremont, CA, USA) for 20 min at 4°C, were labeled with secondary antibody

Alexa Fluor anti-mouse 488 (1:50, Thermo Fisher Scientific) for 20 min at 4°C. Cells were analyzed with Epics XL flow cytometer (Beckman Coulter).

Skin reconstructs

Reconstructs were obtained by seeding human keratynocytes and melanoma cells on dermal equivalents generated by fibroblasts induced type I collagen contraction, as described in Supplementary Materials.

Western Blotting

Spheroids were harvested 48 or 72 h after seeding and WB was performed as previously described (Tiberio et al., 2002) and indicated in Supplementary Materials.

Immunohistochemistry

Skin reconstructs and skin lesions were stained with hematoxylin and eosin (H&E), S100 (1:400; Dako, Agilent Technologies, Dako Denmark A/S, Glostrup, Denmark), CD271 (1:100 in PBS, Lab Vision Corporation), ABCB5 (1:100 in PBS, Thermo Scientific), Hif-1α (1:50 in PBS, Novus, Cambridge, UK) and Oct4 (1:100, Abcam, Cambridge, UK) as described in Supplementary Materials. Spheroids in collagen I were fixed in 4% formalin for 30 minutes before CD271 detection. Sorted cells were fixed and stained with Slug (1:100, Histo-Line Laboratories, Milano, Italy) and Oct4 (1.100, Abcam) as indicated in Supplementary materials.

Cell sorting

Cells were sorted for CD271 expression by Facs sorter as described in Supplementary Materials.

Cells transfection

Cells plated for 24 h in antibiotic-free medium were transfected with CD271 or scrambled siRNA (Dharmacon Inc, Lafayette, CO, USA) in antibiotic/FBS-free medium, supplemented with 0.1% BSA as previuosly described (Truzzi et al., 2011) and indicated in Supplementary Materials.

Cells infection

Spheroids were transduced by infection with viral supernatant generated by CD271-LNSN packaging cells or by empty vector packaging cells (kindly provided from F. Mavilio) as described in Supplementary Materials.

Apoptosis evaluation

For Tunel assay, spheroids were fixed in paraformaldehyde 4% and cytospinned. Slides were stained with the "In situ cell death detection kit" (Roche Diagnostics, Basel, Switzerland) and analyzed by confocal laser microscopy as described in Supplementary Materials. Spheroids were trypsinized and stained with propidium iodide (Milano, Italy) at different time point, as indicated in Supplementary material.

Zebrafish

Larvae were injected at 2 days post fertilization with melanoma cells as indicated in Supplementary materials.

Cell-Cell adhesion assay

Cell adhesion assay was performed as previously described (Quian et al., 1994) and indicated in Supplementary materials.

Statistical analysis

The Student's t-test was used, as indicated in Supplementary Materials.

Conflict of interest:

The authors declare no conflict of interest.

Acknowledgements

This work was partially supported by Fondazione Cassa di Risparmio di Modena, Italy. We thank Prof Massimo Dominici for the advice in cell sorting. Natascia Tiso is supported by AFM-Telethon (Project 18572 Polygon) and EU ZF-HEALTH, Italian Ministry of Health (RF-2010-2309484)

REFERENCES

Beaumont KA, Kumaran NM, Haass NK. Modeling Melanoma In Vitro and In Vivo. Healthcare 2014;2:27-46.

Blochl A, Blochl R. A cell-biological model of p75NTR signaling. J Neurochem 2007;102:289–305.

Boiko AD, Razorenova OV, van de Rijn M, Swetter SM, Johnson DL, Ly DP, et al. (2010) Human melanoma-initiating cells express neural crest nerve growth factor receptor CD271. Nature 2010;466:133-7.

Carlsson J, Yuhas JM. Liquid-overlay culture of cellular spheroids. Recent Results Cancer Res 1984;95:1-23.

Cheli Y, Bonnazi VF, Jacquel A, Allegra M, De Donatis GM, Bahadoran P, et al. CD271 is an imperfect marker for melanoma initiating cells. Oncotarget 2014;5:5272-83.

Civenni G, Walter A, Kobert N, Mihic-Probst D, Zipser M, Belloni B, et al. Human CD271-positive melanoma stem cells associated with metastasis establish tumor heterogeneity and long-term growth. Cancer Res 2011;71:3098-109.

Dallaglio K, Petrachi T, Marconi A, Truzzi F, Lotti R, Saltari A, et al. Expression of nuclear survivin in normal skin and squamous cell carcinoma: a possible role in tumour invasion. Br J Cancer 2014;110:199-207.

De Wever O, Hendrix A, De Boecj A, Westbroek W, Braems G, et al. Modeling and quantification of cancer cell invasion through collagen type I matrices. Int J Dev Biol 2010;54:887-96.

De Witt Hamer PC1, Leenstra S, Van Noorden CJ, Zwinderman AH. Organotypic glioma spheroids for screening of experimental therapies: how many spheroids and sections are

required? Cytometry A 2009;75:528-34.

Donato AL, Huang Q, Liu X, Li F, Zimmerman MA, Li CY. Caspase 3 promotes surviving melanoma tumor cell growth after cytotoxic therapy. J Invest Dermatol 2014;134:1686-92.

Eggermont AM, Spatz A, Robert C. Cutaneous melanoma. Lancet 2014;383:816-27.

Fenouille N, Tichet M, Dufies M, Pottier A, Mogha A, Soo JK, et al. The epithelial-Mesenchymal Transition (EMT) regulatory factor SLUG (SNAI2) is a downstream target of SPARC and AKT in promoting melanoma cell invasion. PLoS One 2012;7:e40378.

Ghosh S1, Spagnoli GC, Martin I, Ploegert S, Demougin P, Heberer M, et al. Three-dimensional culture of melanoma cells profoundly affects gene expression profile: a high density oligonucleotide array study. J Cell Physiol 2005;204:522-31.

Gray-Shopfer V, Wellbrock C, Marias R. Melanoma biology and new targeted therapy. Nature 2007;445:851-7.

Griffith LG, Swarz MA. Capturing complex 3D tissue physiology in vitro. Nat Rev Mol Cell Biol 2006;7:211-24.

Heilmann S, Ratnakumar K, Langdon EM, Kansler ER, Kim IS, Campbell NR, et al. A Quantitative System for Studying Metastasis Using Transparent Zebrafish. Cancer Res 2015; 75:4272–82.

Kaufman CK, Mosimann C, Fan ZP, Yang S, Thomas A, Ablain J, et al. A zebrafish melanoma model reveals emergence of neural crest identity during melanoma initiation. Science 2016;351:aad2197.

Khwaja F, Allen J, Lynch J, Andrews P, Djakiew D. Ibuprofen inhibits survival of bladder cancer cells by induced expression of the p75NTR tumor suppressor protein. Cancer Res 2004;64:6207-13.

Kimmel CB1, Ballard WW, Kimmel SR, Ullmann B, Schilling TF. Stages of embryonic

development of the zebrafish. Dev Dyn 1995;203:253-310.

Kraemer BR, Snow JP, Vollbrecht P, Pathak A, Valentine WM, Deutch AY, et al. A role for the p75 neurotrophin receptor in axonal degeneration and apoptosis induced by oxidative stress. J Biol Chem 2014;289:21205-16.

Kruger GM, Mosher JT, Bixby S, Joseph N, Iwashita T, Morrison SJ, et al. Neural crest stem cells persist in the adult gut but undergo changes in self-renewal, neuronal subtype potential, and factor responsiveness. Neuron 2002;35:657-69.

Liu YR, Sun B, Zhao XL, Gu Q, Liu ZY, Dong XY, et al. Basal caspase-3 activity promotes migration, invasion, and vasculogenic mimicry formation of melanoma cells. Melanoma Res 2013;23:245-53.

Marchetti D, Parikh N, Sudol M, Gallick GE. Stimulation of the protein tyrosine kinase c-Yes but not c-Src by neurotrophins in human brain-metastatic melanoma cells. Oncogene 1998;16:3253-3260.

Marconi A, Borroni RG, Truzzi F, Longo C, Pistoni F, Pellacani G, et al. Hypoxia-Inducible Factor-1α and CD271 inversely correlate with melanoma invasiveness. Exp Dermatol 2015;5:396-8.

Menon DR, Das S, Krepler C, Vultur A, Rinner B, Schauer S, et al. A stress-induced early innate response causes multidrug tolerance in melanoma. Oncogene 2015;34:4545.

Qian F, Vaux DL, Weissman IL. Expression of the integrin alpha 4 beta 1 on melanoma cells can inhibit the invasive stage of metastasis formation. Cell 1994;77:335-47.

Quintana E1, Shackleton M, Foster HR, Fullen DR, Sabel MS, Johnson TM, et al. Phenotypic heterogeneity among tumorigenic melanoma cells from patients that is reversible and not hierarchically organized. Cancer Cell 2010;18:510-23.

Ramgolam K, Lauriol J, Lalou C, Lauden L, Michel L, de la Grange P, et al. Melanoma spheroids grown under neural crest cell conditions are highly plastic migratory/invasive tumor cells

endowed with immunomodulator function. PLoS One 2011;6:e18784.

Selimovic D, Sprenger A, Hannig M, Haïkel Y, Hassan M. Apoptosis related protein-1 triggers melanoma cell death via interaction with the juxtamembrane region of p75 neurotrophin receptor. J Cell Mol Med 2012;6:349-361.

Shirley SH, Greene VR, Duncan LM, Torres Cabala CA, Grimm EA, Kusewitt DF. Slug expression during melanoma progression. Am J Pathol 2012;180:2479-89.

Tiberio R, Marconi A, Fila C, Fumelli C, Pignatti M, Krajewski S, et al. Keratinocytes enriched for stem cells are protected from anoikis via an integrin signaling pathway in a Bcl-2 dependent manner. FEBS Lett 2002;524:139-44.

Truzzi F, Marconi A, Lotti R, Dallaglio K, French LE, Hempstead BL, et al. Neurotrophins and their receptors stimulate melanoma cell proliferation and migration. J Invest Dermatol 2008;128:2031-40.

Truzzi F, Marconi A, Atzei P, Panza MC, Lotti R, Dallaglio K, et al. p75 neurotrophin receptor mediates apoptosis in transit-amplifying cells and its overexpression restores cell death in psoriatic keratinocytes. Cell Death Differ 2011;18:948-58.

Vörsmann H, Groeber F, Walles H, Busch S, Beissert S, Walczak H, et al. Development of a human three-dimensional organotypic skin-melanoma spheroid model for in vitro drug testing. Cell Death Dis 2013;4:e719.

Westerfield M. The zebrafish book. A guide for the laboratory use of zebrafish (Danio rerio). Eugene: University of Oregon Press; 2000.

White R, Rose K, Zon L. Zebrafish cancer: the state of the art and the path forward. Nat Rev Cancer 2013;13:624-36.

FIGURE LEGENDS

Figure 1. CD271 inversely correlates with melanoma progression stage and invasiveness in 3D spheroids. (A) Melanoma cells obtained from spheroids were immunostained with anti-CD271 MoAb and analyzed by flow cytometry. (B) Spheroids were harvested, cytospinned and immunohistochemical detection of Ki67 was performed by using Fast Red as cromogen. The number of positive cells was counted in six independent fields, and Ki67 level was calculated as the average percentage of positive cells. (C) Cells isolated from melanoma biopsies were used to obtain freshly isolated cells and spheroids grown up to 168 h. Cells were cytospinned and immunohistochemistry of different markers was performed. Scale bar = 50μm (D) the percentage of positive cells in spheroids and in freshly isolated cells was compared with the same skin lesion (E) Cells freshly isolated from a primary and a metastatic tumor were cultured as 3D spheroids and MTT assay was performed at different times. (F) Pictures of spheroids implanted into type I collagen were analyzed and (G) total areas were calculated by using ImageJ (see M&M). (H) 20 spheroids for cell line were stained with anti-CD271 MoAb for 3D confocal analysis. Scale bar = 100∝m (I) Proteins extracted from melanoma spheroids 168 h after seeding were immunoblotted with CD271, Survivin, HIF-1α, Notch1, Caspase-3 and β-Actin Ab. The band intensity was quantitatively determined using ImageJ software (Wayne Rasband, see graph and M&M). Protein levels' intensity was normalized to β-actin expression. * $0.01<p<0.05$; ** $p<0.01$. (L) Spheroids were implanted into a scaffold of type I collagen and (M) Pixel analysis was performed to calculate total area. Data represent the mean ± S.D. of triplicate determinations and T-Student was used for statistical analysis.

Figure 2. CD271 is associated with poor invasiveness in spheroids and skin equivalents (A) Melanoma spheroids were implanted into type I collagen, and stained 72 h later with CD271 MoAb. Fast Red was used as cromogen. Cells were counted using ImageJ (see M&M) (B) Pictures were used to count $CD271^+$ cells (red), and $CD271^-$ cells (arrows). Scale bars = 30∝m (right) and 120∝m (left, zoom). (C) "Invading cells" are all the cells outside the spheroid and embedded in collagen I. "Non invading cells" are those located within the body of the sphere. Among invasive cells, $CD271^+$ and $CD271^-$ cells were counted. Data represent the mean ± S.D. of triplicate determinations, and T-Student was used for statistacal analysis. * $0.01 < p < 0.05$; ** $p<0.01$ (D) Skin reconstructs obtained as described in M&M, were paraffin-embedded after either 6 or 12 days of submersion. Sections were stained with H&E, CD271 and S100 MoAb. Fast red for CD271 or DAB for S100 were used as cromogen. Scale bar = 100∝m.

Figure 3. CD271$^-$ spheroids display increased proliferation and invasion abilities (A) CD271$^+$ and CD271$^-$ SKMEL28 subpopulations were cultured up to 168 h after seeding, and MTT assay was performed at different times. (B) Pictures of spheroids were converted to 8-bit, and (C) were analyzed with ImageJ for the calculation of total area (see M&M). (D) CD271$^+$ and CD271$^-$ cells were grown for 7 days as spheroids, dissociated, counted and replated under the same conditions in a long-term assay. (E) CD271$^+$ and CD271$^-$ cells were fixed and cytospinned immediatedly after cell sorting. Immunohistochemical detection of Oct4 was performed by using Fast Red as cromogen. The number of positive cells was counted in six independent fields, and Oct4 level was calculated as the average percentage of positive cells. (F) Pictures of CD271$^+$ and CD271$^-$
SKMEL28 spheroids implanted into type I collagen were analyzed up to 120h, and factor shape, percentage of fragmentation and (G) total areas were calculated by using ImageJ (see M&M). (H) Total number of invading cells was counted with the ImageJ "Cell Counter" (see M&M). (I) Distances reached by the cells in type I collagen was evaluated by using Photoshop, considering cells migrated in the directions of the four cardinal points. The average distance was calculated and the number of pixels were converted into micron (see M&M). (L) Immunoistochemical detection of Slug was performed after cell sorting. The percentage of positive cells was calculated by counting six independent fields. Data represent the mean of triplicate determinations. T-Student was used for statistacal analysis. * $0.01 < p < 0.05$; ** $p<0.01$

Figure 4. CD271 silencing enhances proliferation and invasiveness in melanoma spheroids.
(A) WM115 cells were transfected with 50nM CD271 siRNA, and protein extracts were immunoblotted with CD271 and survivin MoAb. The band intensity was quantitatively determined using ImageJ software (Wayne Rasband, see graph and M&M). Protein levels' intensity was normalized to β-actin expression. * $0.01<p<0.05$; ** $p<0.01$. (B, C) Pictures of spheroids were converted in 8-bit and (C) pixel analysis was performed with ImageJ to calculate total area (see M&M). (D) MTT assay at different times. (E) WM115 cells were transfected with scramble and CD271siRNA and seeded as spheroids. 72 h after, spheroids were implanted into type I collagen and pictures were taken at different times. (F) Factor shape and the percentage of fragmentation were calculated (see M&M). (G) Pixel analysis was performed to calculate total area (see M&M). (H) Invading cells were counted with ImageJ (see M&M). (I) Distances reached by cells in type I collagen were evaluated (see M&M). Data represent the mean ± S.D. of triplicate determinations. T-Student was used for statistical analysis. * $0.01 < p < 0.05$; ** $p<0.01$.

Figure 5. CD271 overexpression decreases tumor proliferation and invasiveness in melanoma spheroids (A) SKMEL28 were infected with mock or CD271 retroviral vector, and cell lysates were immunoblotted. The band intensity was quantitatively determined using ImageJ software (Wayne Rasband, see graph and M&M). Protein levels' intensity was normalized to β-actin expression. * $0.01<p<0.05$; ** $p<0.01$. (B) SKMEL28 spheroids pictures were converted with ImageJ. (C) Pixel analysis was performed to calculate total areas (see M&M) . (D) MTT assay. (E, F) Apoptotic cells of SKMEL28 mock and CD271 infected spheroids was evaluated by Tunel and PI assay. (G) CD271 infected and mock treated spheroids were implanted into a scaffold of type I collagen. Factor shape, percentage of fragmentation, (H) total area and (I) invasion area were calculated (see M&M). (L) Distances reached by SKMEL28 cells into type I collagen. The average distance was calculated (see M&M). Data represent the mean ± S.D. of triplicate determinations. T-Student was used for statistical analysis. * $0.01 < p < 0.05$; ** $p<0.01$.

Figure 6. The lack of CD271 favours tumor metastasis in zebrafish and is associated with a reduced cell-cell adshesion. (A) $CD271^+$ and $CD271^-$ SKMEL28 subpopulations were stained with Vybrant Cell Labeling Solution (red), injected into the yolk of transparent zebrafish larvae at 2days post fertilization (2dpf) and monitored. (B) The number of embryos with metastasis was counted at 1day and 6days post injection (1dpi and 6dpi). (C) The percentage of zebrafish with "Full metastasis" (>10 cells), "medium metastasis" (5-10 cells) and "initial metastasis" (2-4 cells) was calculated; (D) SKMEL28 $CD271^+$ (green, stained with CFSE) and $CD271^-$ (red, stained with Vybrant-Cell Labeling Solution) cells were injected together in zebrafish larvae and pictures were taken at 2dpi and 7dpi; (E) WM115 scramble and CD271 siRNA cells (red) were injected into zebrafish at 2dpf and (F) the number and (G) the severity of metastasis were calculated at 2dpi and 7dpi; (H) 1205Lu mock and CD271 infected cells (red) were injected into transparent larvae. (I) The percentage of metastasis was calculated at 1dpi and 6 dpi. (L) "Full", "medium" and "initial" metastasis were evaluated. (M, N) Proteins extracted from melanoma spheroids 168h after seeding were immunoblotted with β_1-integrin and β-actin. The band intensity was quantitatively determined using ImageJ software (Wayne Rasband, see graph and M&M). Protein levels' intensity was normalized to β-actin expression. * $0.01<p<0.05$; ** $p<0.01$. (O) For the cell-cell adhesion assay, the same cells were stained with Vybrant-Cell Labeling Solution (red) and CFSE (green). WM115 scramble and CD271 siRNA cells stained with CFSE (green) were grown as monolayer. WM115 scramble and CD271 siRNA cells stained with Vybrant-Cell Labeling Solution (red) were plated on the corresponding monolayer and incubated for 40 minutes at 37^o C. After washing the unbound cells, the number of red cells/mm^2 were counted

(see M&M). The same experiment was performed for 1205Lu mock and CD271 infected cells.

Scale bar = 20μm

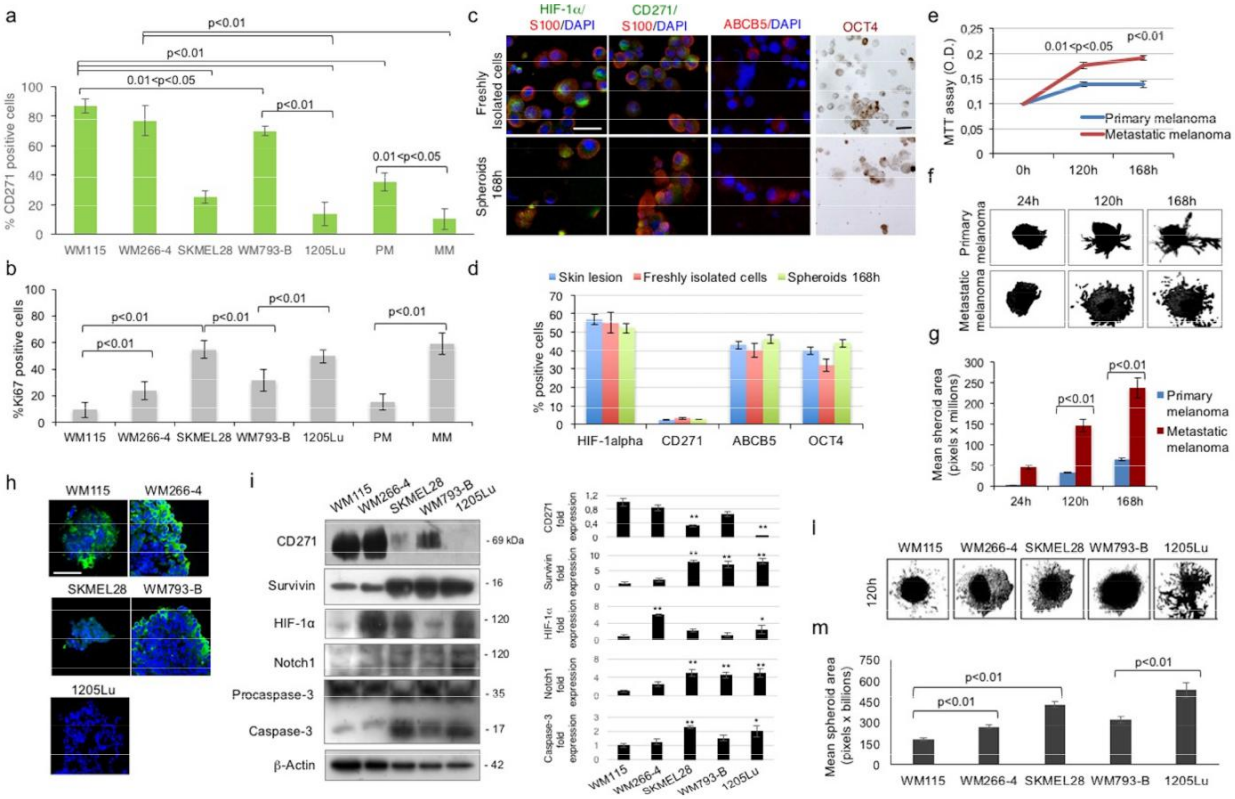
a
% CD271 positive cells
p<0.01
p<0.01
0.01<p<0.05
p<0.01
0.01<p<0.05
WM115 WM266-4 SKMEL28 WM793-B 1205Lu PM MM
b
%Ki67 positive cells
p<0.01
p<0.01
p<0.01
p<0.01
WM115 WM266-4 SKMEL28 WM793-B 1205Lu PM MM
c
HIF-1α/ S100/DAPI
CD271/ S100/DAPI
ABCB5/DAPI
OCT4
Freshly Isolated cells
Spheroids 168h
d
Skin lesion
Freshly isolated cells
Spheroids 168h
% positive cells
HIF-1alpha CD271 ABCB5 OCT4
e
MTT assay (O.D.)
0.01<p<0.05
p<0.01
Primary melanoma
Metastatic melanoma
0h 120h 168h
f
24h 120h 168h
Primary melanoma
Metastatic melanoma
g
Mean sheroid area (pixels x millions)
p<0.01
p<0.01
Primary melanoma
Metastatic melanoma
24h 120h 168h
h
WM115 WM266-4
SKMEL28 WM793-B
1205Lu
i
WM115 WM266-4 SKMEL28 WM793-B 1205Lu
CD271 - 69 kDa
Survivin - 16
HIF-1α - 120
Notch1 - 120
Procaspase-3 - 35
Caspase-3 - 17
β-Actin - 42
CD271 fold expression
Survivin fold expression
HIF-1α fold expression
Notch1 fold expression
Caspase-3 fold expression
WM115 WM266-4 SKMEL28 WM793-B 1205Lu
l
120h
WM115 WM266-4 SKMEL28 WM793-B 1205Lu
m
Mean spheroid area (pixels x billions)
p<0.01
p<0.01
p<0.01
WM115 WM266-4 SKMEL28 WM793-B 1205Lu

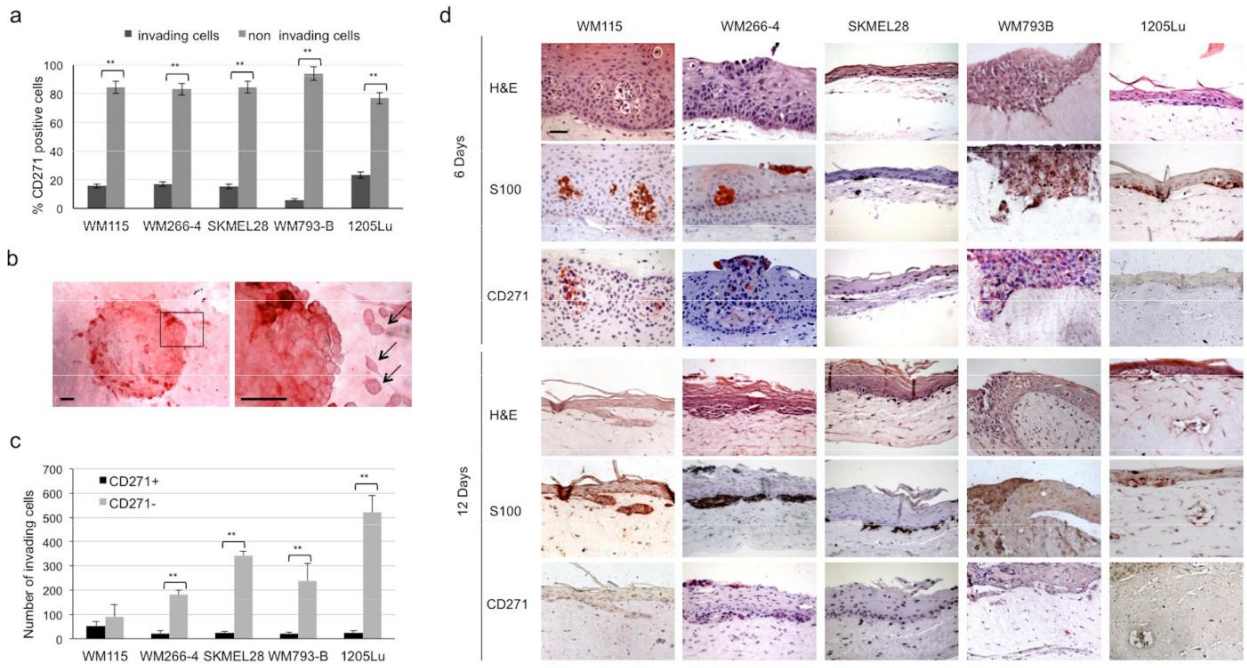
a
invading cells
non invading cells
% CD271 positive cells
WM115
WM266-4
SKMEL28
WM793-B
1205Lu
b
c
CD271+
CD271-
Number of invading cells
d
WM115
WM266-4
SKMEL28
WM793B
1205Lu
6 Days
12 Days
H&E
S100
CD271

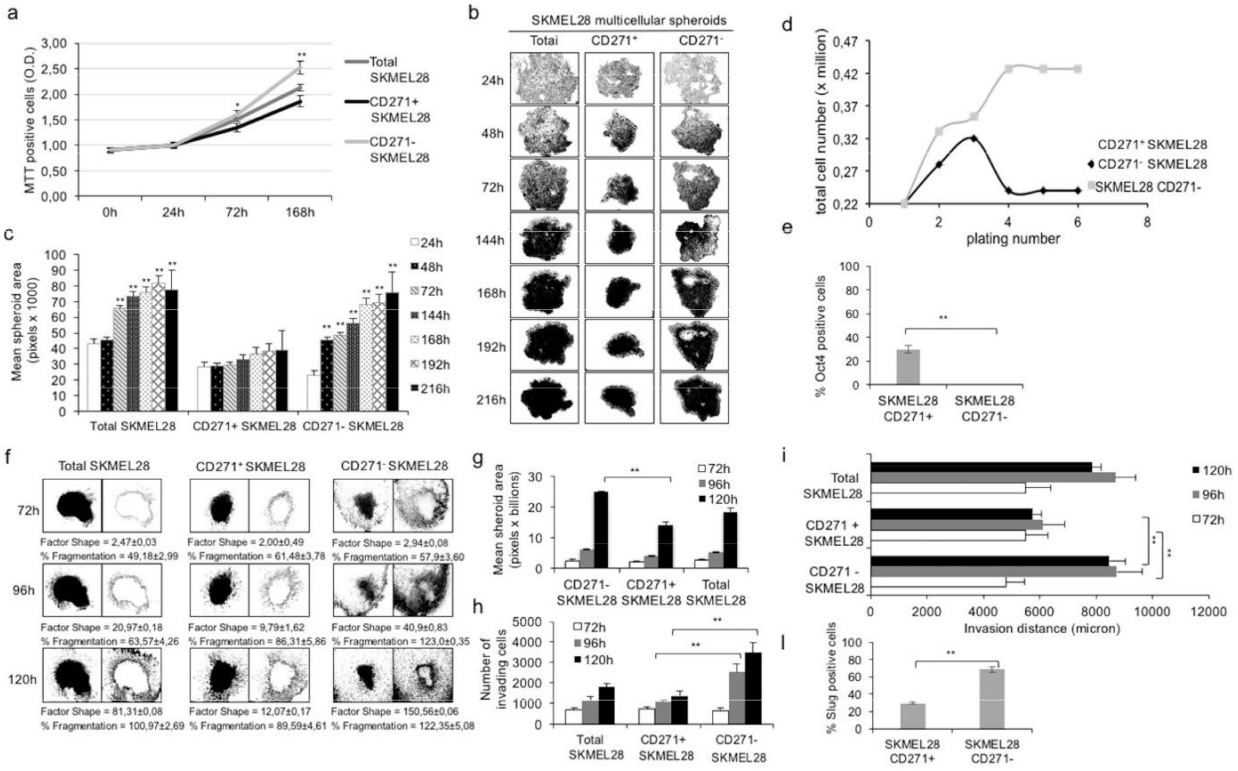
a
MTT positive cells (O.D.)
Total SKMEL28
CD271+ SKMEL28
CD271- SKMEL28
0h
24h
72h
168h
b
SKMEL28 multicellular spheroids
Totai
CD271+
CD271-
24h
48h
72h
144h
168h
192h
216h
c
Mean spheroid area (pixels x 1000)
24h
48h
72h
144h
168h
192h
216h
Total SKMEL28
CD271+ SKMEL28
CD271- SKMEL28
d
total cell number (x million)
plating number
CD271+ SKMEL28
CD271- SKMEL28
SKMEL28 CD271-
e
% Oct4 positive cells
SKMEL28 CD271+
SKMEL28 CD271-
f
Total SKMEL28
CD271+ SKMEL28
CD271- SKMEL28
72h
96h
120h
Factor Shape = 2,47±0,03
% Fragmentation = 49,18±2,99
Factor Shape = 2,00±0,49
% Fragmentation = 61,48±3,78
Factor Shape = 2,94±0,08
% Fragmentation = 57,9±3,60
Factor Shape = 20,97±0,18
% Fragmentation = 63,57±4,26
Factor Shape = 9,79±1,62
% Fragmentation = 86,31±5,86
Factor Shape = 40,9±0,83
% Fragmentation = 123,0±0,35
Factor Shape = 81,31±0,08
% Fragmentation = 100,97±2,69
Factor Shape = 12,07±0,17
% Fragmentation = 89,59±4,61
Factor Shape = 150,56±0.06
% Fragmentation = 122,35±5,08
g
Mean sheroid area (pixels x billions)
72h
96h
120h
CD271- SKMEL28
CD271+ SKMEL28
Total SKMEL28
h
Number of invading cells
72h
96h
120h
Total SKMEL28
CD271+ SKMEL28
CD271- SKMEL28
i
Total SKMEL28
CD271 + SKMEL28
CD271 - SKMEL28
120h
96h
72h
Invasion distance (micron)
l
% Slug positive cells
SKMEL28 CD271+
SKMEL28 CD271-

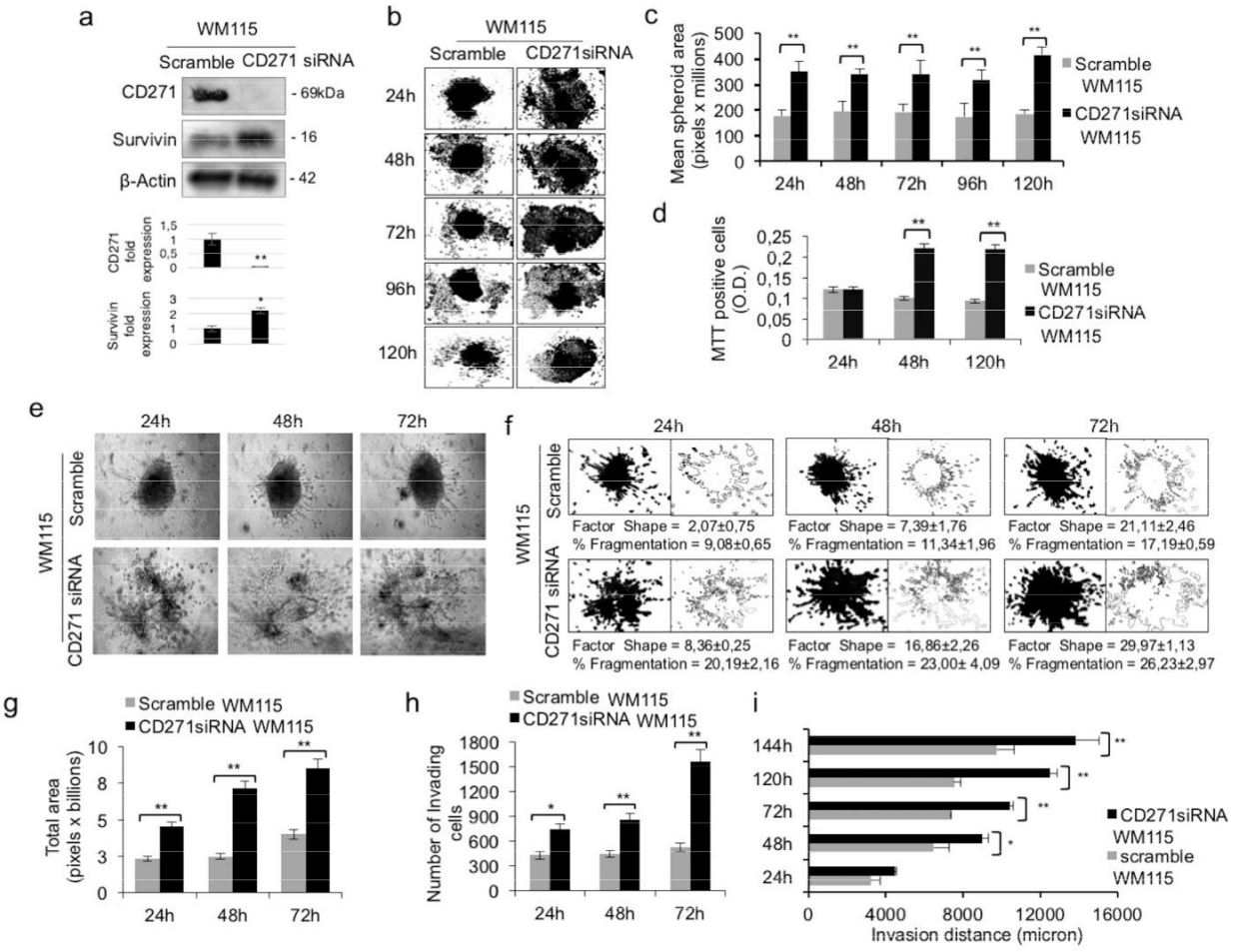
a
WM115
Scramble CD271 siRNA
CD271
- 69kDa
Survivin
- 16
β-Actin
- 42
CD271 fold expression
Survivin fold expression
b
WM115
Scramble CD271siRNA
24h
48h
72h
96h
120h
c
Mean spheroid area (pixels x millions)
Scramble WM115
CD271siRNA WM115
24h 48h 72h 96h 120h
d
MTT positive cells (O.D.)
Scramble WM115
CD271siRNA WM115
24h 48h 120h
e
24h 48h 72h
WM115
Scramble
CD271 siRNA
f
24h 48h 72h
WM115
Scramble
CD271 siRNA
Factor Shape = 2,07±0,75
% Fragmentation = 9,08±0,65
Factor Shape = 7,39±1,76
% Fragmentation = 11,34±1,96
Factor Shape = 21,11±2,46
% Fragmentation = 17,19±0,59
Factor Shape = 8,36±0,25
% Fragmentation = 20,19±2,16
Factor Shape = 16,86±2,26
% Fragmentation = 23,00± 4,09
Factor Shape = 29,97±1,13
% Fragmentation = 26,23±2,97
g
Scramble WM115
CD271siRNA WM115
Total area (pixels x billions)
24h 48h 72h
h
Scramble WM115
CD271siRNA WM115
Number of Invading cells
24h 48h 72h
i
144h
120h
72h
48h
24h
CD271siRNA WM115
scramble WM115
Invasion distance (micron)

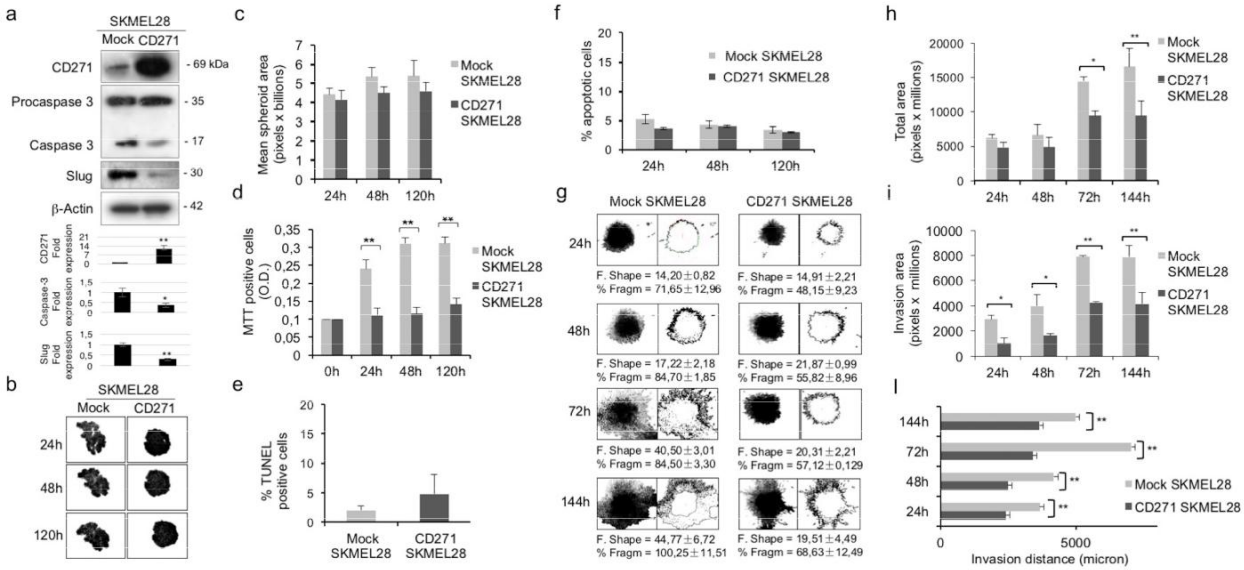
a
SKMEL28
Mock CD271
CD271
Procaspase 3
Caspase 3
Slug
β-Actin
- 69 kDa
- 35
- 17
- 30
- 42
CD271 Fold expression
Caspase-3 Fold expression
Slug Fold expression
b
SKMEL28
Mock
CD271
24h
48h
120h
c
Mean spheroid area (pixels x billions)
Mock SKMEL28
CD271 SKMEL28
24h
48h
120h
d
MTT positive cells (O.D.)
Mock SKMEL28
CD271 SKMEL28
0h
24h
48h
120h
e
% TUNEL positive cells
Mock SKMEL28
CD271 SKMEL28
f
% apoptotic cells
Mock SKMEL28
CD271 SKMEL28
24h
48h
120h
g
Mock SKMEL28
CD271 SKMEL28
24h
F. Shape = 14,20±0,82
% Fragm = 71,65±12,96
F. Shape = 14,91±2,21
% Fragm = 48,15±9,23
48h
F. Shape = 17,22±2,18
% Fragm = 84,70±1,85
F. Shape = 21,87±0,99
% Fragm = 55,82±8,96
72h
F. Shape = 40,50±3,01
% Fragm = 84,50±3,30
F. Shape = 20,31±2,21
% Fragm = 57,12±0,129
144h
F. Shape = 44,77±6,72
% Fragm = 100,25±11,51
F. Shape = 19,51±4,49
% Fragm = 68,63±12,49
h
Total area (pixels x millions)
Mock SKMEL28
CD271 SKMEL28
24h
48h
72h
144h
i
Invasion area (pixels x millions)
Mock SKMEL28
CD271 SKMEL28
24h
48h
72h
144h
l
144h
72h
48h
24h
Mock SKMEL28
CD271 SKMEL28
0
5000
Invasion distance (micron)

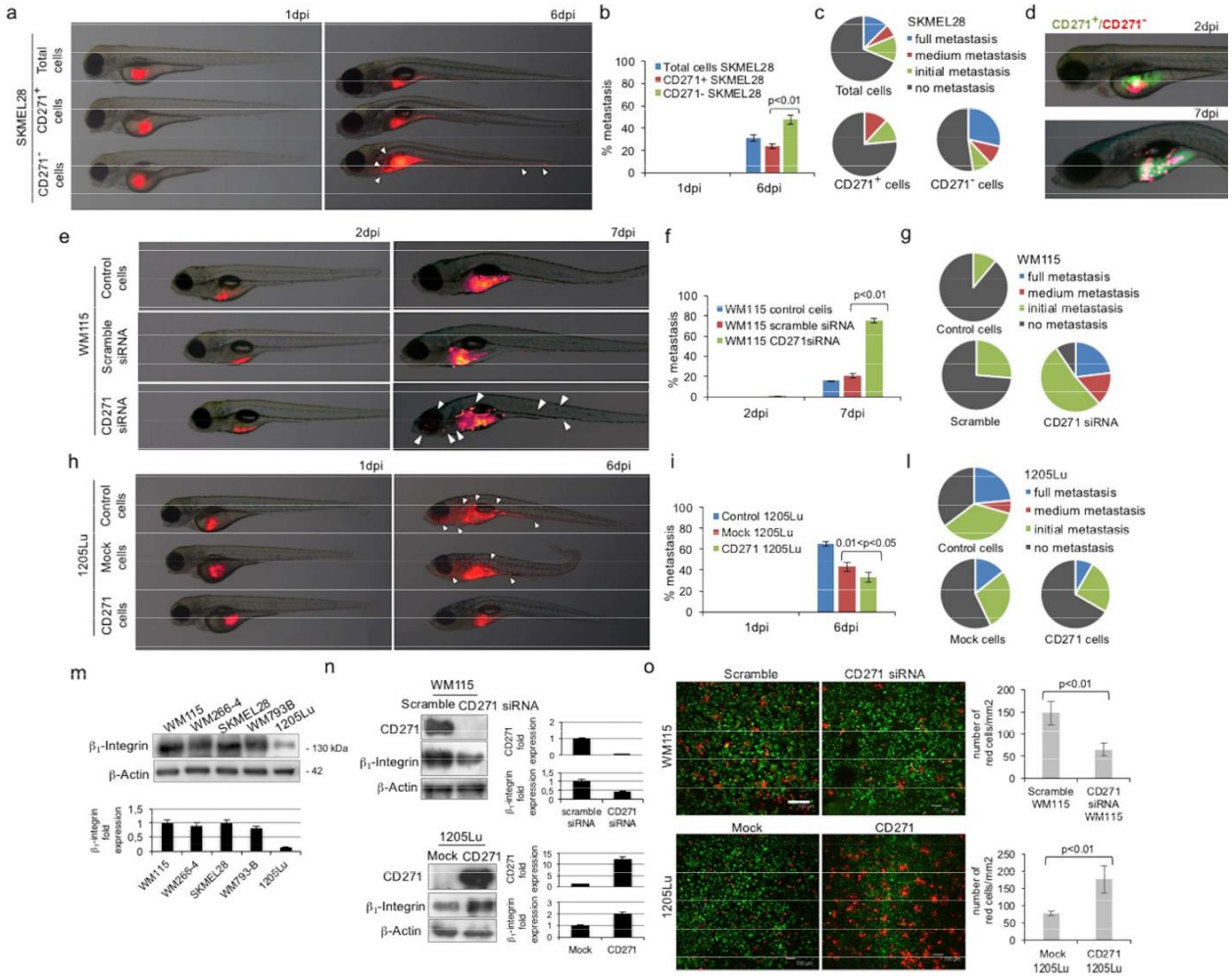
a
1dpi
6dpi
SKMEL28
Total cells
CD271+ cells
CD271- cells
b
Total cells SKMEL28
CD271+ SKMEL28
CD271- SKMEL28
% metastasis
p<0.01
1dpi
6dpi
c
SKMEL28
full metastasis
medium metastasis
initial metastasis
no metastasis
Total cells
CD271+ cells
CD271- cells
d
CD271+/CD271-
2dpi
7dpi
e
2dpi
7dpi
WM115
Control cells
Scramble siRNA
CD271 siRNA
f
WM115 control cells
WM115 scramble siRNA
WM115 CD271siRNA
% metastasis
p<0.01
2dpi
7dpi
g
WM115
full metastasis
medium metastasis
initial metastasis
no metastasis
Control cells
Scramble
CD271 siRNA
h
1dpi
6dpi
1205Lu
Control cells
Mock cells
CD271 cells
i
Control 1205Lu
Mock 1205Lu
CD271 1205Lu
% metastasis
0.01<p<0.05
1dpi
6dpi
l
1205Lu
full metastasis
medium metastasis
initial metastasis
no metastasis
Control cells
Mock cells
CD271 cells
m
WM115
WM266-4
SKMEL28
WM793B
1205Lu
β1-Integrin
β-Actin
130 kDa
42
β1-integrin fold expression
n
WM115
Scramble
CD271 siRNA
CD271
β1-Integrin
β-Actin
CD271 fold expression
β1-integrin fold expression
scramble siRNA
CD271 siRNA
1205Lu
Mock
CD271
Mock
CD271
o
Scramble
CD271 siRNA
WM115
p<0.01
number of red cells/mm2
Scramble WM115
CD271 siRNA WM115
Mock
CD271
1205Lu
p<0.01
Mock 1205Lu
CD271 1205Lu